

# Computational Fluid Dynamic of NACA0012 with LS-DYNA<sup>®</sup> (ALE & ICFD) and Wind Tunnel Tests

B.Perin<sup>1</sup>, O.Verdrel<sup>1</sup>, P.Bordenave<sup>1</sup>, E.Grippon<sup>2</sup>, V.Lapoujade<sup>2</sup>, H.Belloc<sup>3</sup>, I. Caldichoury<sup>4</sup>

<sup>1</sup>DGA Aeronautical Systems, 47 rue Saint Jean, F-31131 Balma Cedex, France

<sup>2</sup>DynaS+, 5 avenue Didier Daurat, F-31400 Toulouse, France

<sup>3</sup>Université de Toulouse / Institut Supérieur de l'Aéronautique et de l'Espace, 10 av. E. Belin, BP 54032, F-31055 Toulouse Cedex 4, France

<sup>4</sup>LSTC, 7374 Las Positas Road, Livermore, CA 94551

## Abstract

DGA Aeronautical Systems, the technical centre of the French ministry of Defense dedicated to aircraft performance testing and evaluation, combines tests and simulations to validate, among others, parachute systems for the Airdrop Department. The latter also developed modeling and simulation capabilities as a support for evaluation. In parallel, under the authority of the French Ministry of Defense, the Department of Aerodynamics, Energetics and Propulsion (DAEP) of Institut Supérieur de l'Aéronautique et de l'Espace (ISAE), a public institution of higher education and research, conducts research and training support for the Institute. As such, it has developed over the last years the research topic "Aerodynamics of Free Flight Devices" focused particularly on paragliding. The DAEP has expertise and resources in the field of wind tunnel tests and flight aerodynamics of paragliders. DynaS+, a LS-DYNA French distributor and associated services, got a research and innovative subvention from French Government, RAPID financing, to improve the parachute simulation with LS-DYNA. All these entities have shared their skills to better understand and to enhance the knowledge of the fluid representation in the Fluid-Structure Interaction (FSI) simulation of parachute models. They have worked to compare different fluid representations from experimental wind tunnel testing to numerical simulations (ALE and ICFD solvers) around a rigid rectangular wing with NACA0012 airfoil. This study is a complementary work from the publication perspective and concerning the simulation of a flexible ram-air. This paper shows the limitations of the ALE solver to get the aerodynamic coefficients for a wing and the hopes raised by the ICFD solver.

## Introduction

Within DGA Aeronautical Systems, the service of numerical simulation of airdrop studies the dynamic behavior of parachutes through simulation performed with LS-DYNA. So far, the ALE solver was predominantly used to get approximate results of parachute aerodynamics and to models flexible ram-air. Despite the absence of turbulence model and the simplified resolution Navier-Stokes equations, this ALE solver allows realizing several studies. For example, a study of a kite (small parachute) has shown very promising results demonstrating the ALE solver's ability to faithfully reproduce the shape of the wing on a wind tunnel [1]. However, this paper has also shown that the ALE calculation gives only approximation of aerodynamic coefficients. This results confirms previous studies on hemispheric parachutes showing an overvaluation of the drag coefficient [2, 3].

Since the R8 version, LS-DYNA has a new ICFD solver for performing multi-physics solicitation. Reassured by the capabilities of the ALE solver to reproduce the shape of a flexible structure in dynamic but aware of the lacks in term of aerodynamic representation of models, DGA Aeronautical Systems wishes to use this new solver.

To consider the regular use of this new solver by the DGA service, a comparison with the ALE solver is necessary, particularly on abilities of the ICFD solver to represent the fluid and its flow. From this point on, DGA Aeronautical Systems and DynaS+ are associated in a methodic analysis of the capabilities of the currently available solvers in order to increase their knowledge

and level of. The convergence of objectives of these two entities is reinforced through the innovative project called PARAFLU carried by DynaS+ and funded by the DGA.

Thus, the purpose of this paper is to compare the two numerical methods ALE and ICFD against experimental wind tunnel results thanks to the DEAP of ISAE. The main characteristics of these two numerical methods are summed up in Table 1:

Name	ALE	ICFD
Application field	Multi-physics (fluid-structure coupling) Explosions, rapid and brief phenomena	Multi-physics (fluid-structure coupling) Internal and External Aerodynamics, High Reynolds flow studies
Methods of numerical discretization spatial	Finite elements	
Solvers type	Compressible	Incompressible
Time integration methods	Explicit	Implicit
Coupling type	Weak	Weak/Strong
Available turbulence models	None	RANS, LES
Possible meshing of boundary layer	No	Yes
Meshes type	Purely hexahedral	Purely tetrahedral

Table 1 – Comparative table between main characteristics of ALE and ICFD solver.

## 1 Presentation of case studies

### 1.1 Choice of Airfoil of aircraft

To allow a meaningful comparison of the performance of the ALE and ICFD solvers and to validate their relevance with theory and experimental tests, a common reference has been selected: study of the flow around a rectangular wing with an airfoil type NACA0012.

This particular NACA is chosen for three reasons: (i) his similar shape with the Airfoil of a ram-air parachute already studied [1] (figure 1), (ii) the possibility to make experimental test in a wind tunnel for this wing and (iii) the multiples references found in literature [4, 5].

System	Airfoil of ram-air parachute	Airfoil of aircraft
Aim of the system	Deceleration	Aerial lift
Airfoil type	Opened	Closed
Surface type	Rough / Porous	Smooth
Material	Fabric	Metallic
Airfoil's picture and dimension	<p>c= 750 mm, l=1000 mm and h=110 mm [1]</p> 	<p>c=298 mm, l=1800 mm and t=c×12%=35.76 mm</p> 

Figure 1 – Comparative table between main characteristics of airfoil of ram-air parachute and aircraft

The problem can be summed up as a resolution of a flow problem around a rigid obstacle, without fluid-structure interaction. This work is part of the longer term goal to improve the fluid solution in the parachute simulation.

### 1.2 Wind tunnel test

The wind tunnel used for these experiments is an elliptical open test section of 3 m wide and 2 m high (Figure 2). The maximum velocity is 40 m/s and turbulence intensity is 0.5% (it's a characteristic data of the vein of the wind tunnel). The results are presented at Reynolds numbers of  $0.84 \times 10^6$ .

The flow is incompressible, subsonic, and transient with little coupling between the structure and the fluid. There is only the action of the fluid on the wing and no sufficient deformation thereof to cause a response which disrupts the aerodynamic field.



Figure 2 – Photos of the standard airfoil NACA0012 setting in the S4 wind tunnel of ISAE.

The reference wing is set on a three masts assembly in the wind tunnel. Moreover, it has added a small tail with a cylinder shape on the back of the wing at level of the trailing edge which allows to give a third point for positioning the wing in the angle of attack. The surface is smooth and the boundary layer transition is left natural. Under the wind tunnel floor, a balance of effort is used to measure the aerodynamic forces applied to the whole system {airfoil + masts}.

The masts are fixed to the floor of the wind tunnel. They pass through the fairings without touching them so that the wind that comes on the fairings is not weighed by the balance. Only the wind which comes on the wing and on the masts is taken into account by the balance. To account and correct for the drag of the masts, a preliminary test without airfoil is made.

Thus, we consider that the aerodynamic forces of the wing are the aerodynamic forces measured during the test with {airfoil + mast} from which we remove the iso-position forces measured on the three masts without airfoil. Thus, the masts are not modeled. Assuming that the lift coefficient  $C_l^{mast} = 0$ , that can be translated on drag coefficient by the equation:

$$C_d^{airfoil}(corrected) = C_d^{airfoil}(with\ masts) - C_d^{masts}$$

where  $C_d$  is the drag coefficient.

Along the aerodynamic axis, the experimental curves of the lift and the drag as function of the angle of attack are compared to the ALE and the ICFD solver. The aerodynamic coefficients are measured for angles of attack ranging from 0 to 20°. The measurement uncertainty on the aerodynamic coefficients is 1%. The measurement uncertainty on the angle of attack is 0.02°. The tests do not contain data on the pressure distributions.

## 2 ALE and ICFD modelling

### 2.1 Common configuration for ALE and ICFD calculations

For both the ALE and ICFD solvers, we consider five angles of attack (Figure 3) (in brackets, the angle of attack measured):

- 0° (0.03°): minimal lift and drag angle;
- 5° (5.23°): angle of trailing edge detachment;
- 10° (10.41°): angle for which the flow become more turbulent and faster transitioning;
- 15° (15.20°): maximal lift with intense detachment but without stall;
- 20° (20.40°): angle in the stall area.

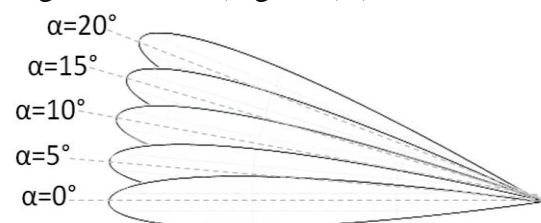


Figure 3 – Schema of the airfoil at different angle of attack.

Note that the maximal glide ratio angle is  $4.3^\circ$ .

Knowing the NACA geometry and the Reynolds number, it is possible to choose:

- 2D or 3D representation: to a first approximation and thanks to the symmetries of the problem, a 2D representation is used for comparison of ALE and ICFD. A 3D representation is also used to perform a parametric study for representative time of calculation.
- the size of the fluid domain is chosen so that the NACA profile is sufficiently far from the boundary conditions. In 2D, the area is  $L \times D = 3 \times 4.5$  m (Figure 4 (b)).
- the mesh size: To determine the order of magnitude of the mesh size near the NACA, the formula of the boundary layer around a flat plate is used:  $\delta = l \times Re^{-1/2} = 3 \times 10^{-3}$  m. A minimum of three elements in the boundary layer is needed to correctly capture this layer. The elements of the mesh layer will be then of the order of  $10^{-3}$  m. So, to avoid having too distorted element along the NACA profile elements, the element size of the profile of the surface mesh vary between  $0.5 \times 10^{-3}$  and  $5 \times 10^{-3}$  m, with a finer mesh at the leading edge in order to better capture the high gradients of pressure there (Figure 4 (a)).
- time step: the order of magnitude of the smallest element is  $10^{-4}$  m and that of the velocity is of  $v = 10^1$  m/s, then the time step is chosen equal to  $5 \times 10^{-5}$  s.
- final time of the study: Without phenomenon of stall or recirculation, the calculation should converge as soon as a virtual particle crossed the domain :  $t = D / v = 4.5 / 40 = 0.11$  s. The final time is chosen 10 times greater, equal to 1s.

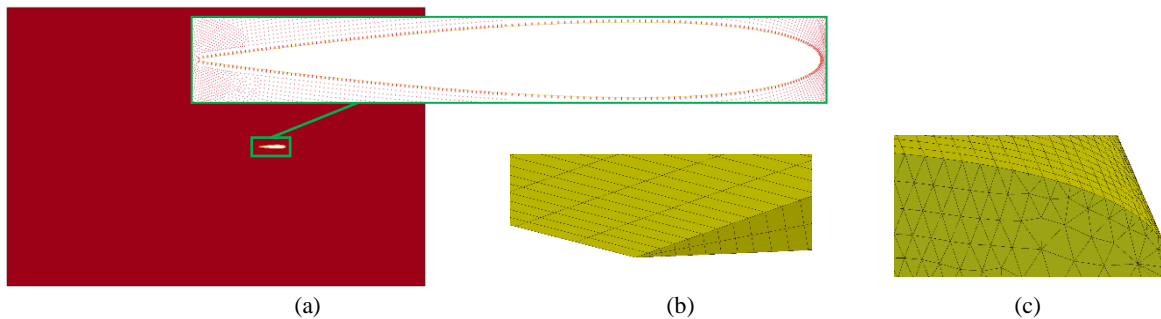


Figure 4 – (a) size of the fluid domain in 2D and discretization of the 2D profile (identical for ALE and ICFD studies) (b) Example of NACA meshing in 3D for ICFD and ALE coarse mesh and (c) ICFD fine mesh.

Velocity and pressure conditions are respectively applied for inflow and outflow conditions. Free slip boundary conditions are applied for the edges of the fluid domain. Non-slip boundary conditions are applied for the Naca.

Simulations have been done with LS-DYNA release R7.1.1 and the R8 dev (SVN version higher than 105806).

## 2.2 ALE introduction and parametric study

The ALE solver of LS-DYNA allows the simulation of three-dimensional flows, unsteady, compressible and without turbulence model and frictional strength. It resolves the modified Navier-Stokes equation in ALE formulation to let the meshing movements. Moreover, it uses the meshing technic of immersed boundaries, that is to say the fluid meshing pass through the structure meshing during its creation. The method of spatial discretization of the equations implemented is the finite volume method adapted to a finite element code. These adaptations from finite element code to calculate flows with a finite volume method led to some adjustments. For example, we can note the introduction of an under-integration method of the solids elements that are ALE or Eulerian to calculate a value of pressure. Consequently, this has introduced

forces of Eulerian viscous Hourglass which can distort the solution and destabilize the calculation if it were not well controlled.

The time integration is explicit and uses the Newark schema. The time step is limited by the CFL condition in which the calculation is based on the characteristic size of the elements and the fluid velocity in a mesh. This condition allows calculating the critical time step and, using a safety factor of 0.9 to decrease it in order to have a stable calculation.

In order to lead an ALE sensitivity on numerical parameters, the model is based on the physical problem of fluid flow around a NACA presented previously, for a 5° angle of attack. Considering a half-model using the symmetrical plane passing through the NACA straight section, the ALE domain has a size of  $4.5 \times 3 \times 1.8\text{m}^3$  (Figure 5). To improve computation time, ALE domain mesh is generated using `*ALE_STRUCTURED_MESH` keyword (about 20% less CPU time compared to classic approach). A 3D model was studied here in order to be representative to a parachute deployment computation. To improve model robustness, a specific ALE Multi-Material Group (AMMG) is used to couple the NACA geometry with the on-going air flow.

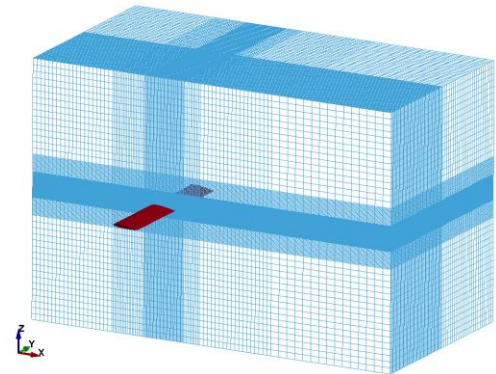


Figure 5: Structured-ALE domain mesh

Multiple parameter configurations were checked (Table 3):

- Penalty coupling parameters: NQUAD, ILEAK;
- Material formulations and equations of state: `*MAT` and `*EOS`;
- Advection method: Donor Cell, Van Leer (METH field in `*CONTROL_ALE` keyword).

<code>*CONSTRAINED_LAGRANGE_IN_SOLID:</code>		<code>*MAT</code>	<code>*CONTROL_ALE :</code>	
CTYPE :	4	<code>*MAT_NULL</code>	NADV :	1
FRCMIN :	0.5	<code>*MAT_ALE_VISCOUS</code>	METH :	1, 2
NQUAD :	2, 3, 4, 5	<code>*MAT_ALE_INCOMPRESSIBLE</code>		
DIREC :	2	<code>*MAT_ALE_MIXING_LENGTH</code>		
ILEAK :	0, 1, 2	<code>*EOS</code>		
PFAC :	0.1	→ LINEAR POLYNOMIAL		
		→ GAS IDEAL		

Table 2: parameter variation for ALE sensitivity study

Changing material and equation of state has not shown significant influence on drag and lift forces despite computation time. Viscous effect on NACA interaction surface has not been modeled: no frictional coefficient equivalent to viscous effect on interface has been set.

Using `*MAT_NULL` coupling with linear polynomial EOS, a LS-OPT<sup>®</sup> model to identify the influence of ILEAK, METH and NQUAD has been set.

Firstly, regarding influence of ILEAK parameter on drag force (Figure 6), results show a more stable solution by setting ILEAK to 0 in the context of this study.

Modifying advection method (METH) does not show real impact on the results.

The sliding energy level and the ratio between Hourglass energy and intern energy were checked as validation criteria. It appears that it is better to increase the FRCMIN and NQUAD settings to improve the results of the drag coefficients. However, there is an insensitivity of results on the lift coefficient.

Considering a Donor Cell advection method and leakage control deactivated, setting  $NQUAD \geq 4$  gives quite the same results, for the considered mesh size (Figure 7). An increase of  $NQUAD$  has the effect to increase the coupling pressure and makes the calculation more conservative.

Parameters identify here are often recommended while setting a FSI study with ALE solver. However, depending on the physical phenomenon, other value parameters could be better.

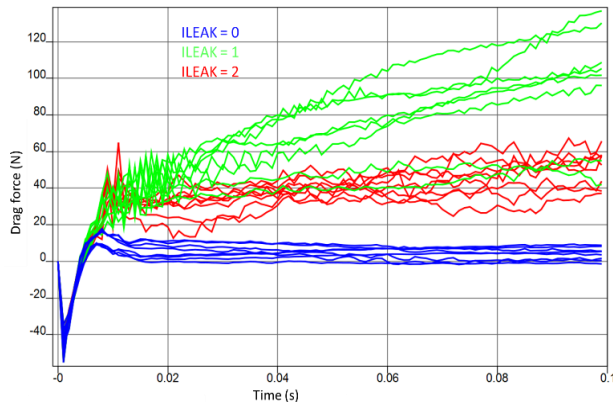


Figure 6: ILEAK influence on drag force

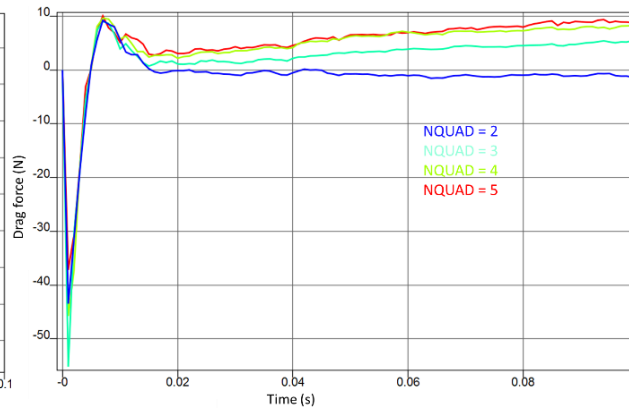


Figure 7: NQUAD influence on drag force

### 2.3 ICFD introduction and parametric study

The ICFD solver allows the simulation in two and three dimensional, unsteady, incompressible and viscous fluid, laminar and turbulent flow with models type RANS and LES. It uses the method of prediction-correction (fractional step method) for achieving the velocity-pressure coupling to enhance the condition of incompressibility. The integration is implicit with a finite difference method of backward type of second order [6, 7]. Compared with explicit solvers, here there is the notion of convergence of the solution at each time step that is added and we are no longer constrained by the CFL condition. So, it can have more refined meshes without drastically reducing the time step.

The solver is purely tetrahedral for the fluid. The mesh generation is automatic. The greater part of the analysis of ICFD performance in this paper is focused on the study of mesh convergence near the structure and for the volume control. The study with the ICFD Solver allowed assessing the influence of these following points:

- the size of the fluid domain (Figure 8); Three fluid domain sizes were tested.
- the fluid meshing near the NACA (Figure 9); two discretization of the NACA were evaluated (Figure 9 (a) and (b)). The influence of finer boxing was test (Figure 9 (a), (b) and (c)).
- the mesh in the boundary layer: \*MESH\_BL; tests without and with a coarse or fine refinement of the boundary layer were tested.
- the turbulent flow model. Different formulations of the k- $\epsilon$  model are tested (RANS model);

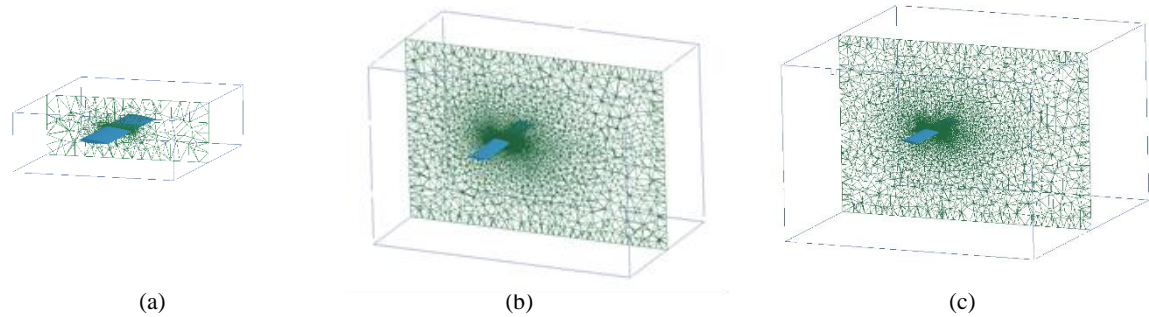


Figure 8 – Fluid domain size: (a)  $1.7 \times 2.6 \times 0.6 \text{ m}^3$ , (b)  $4.5 \times 2.8 \times 3 \text{ m}^3$  and (c)  $4.5 \times 4.8 \times 3 \text{ m}^3$

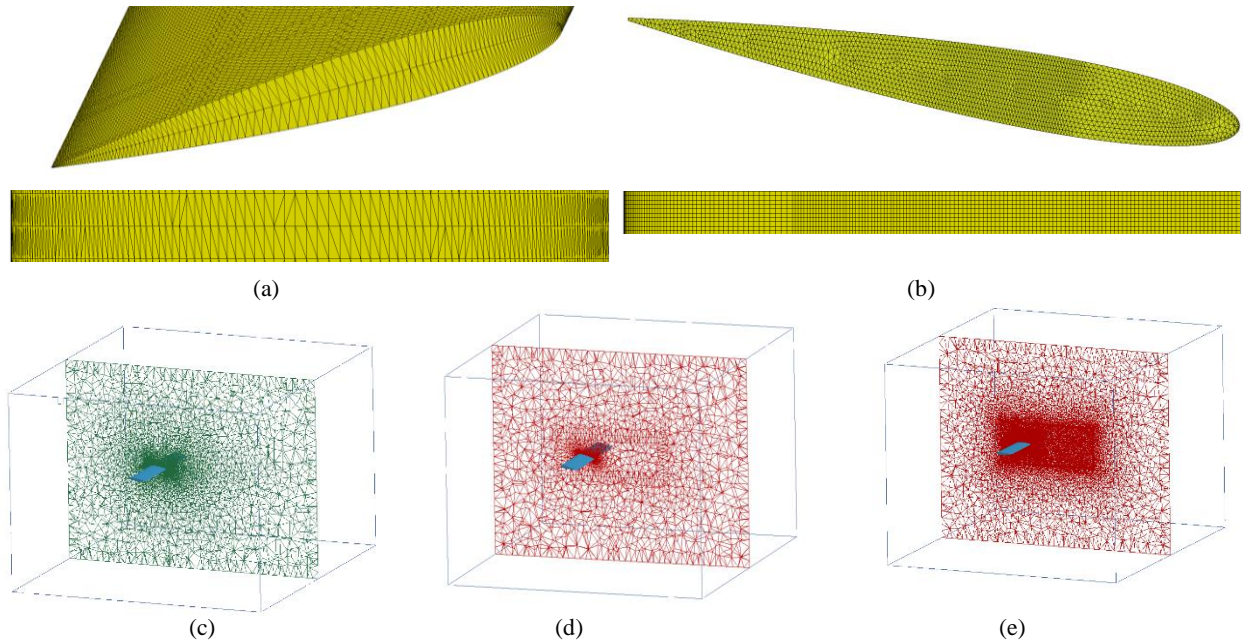


Figure 9 – Different meshing of the structure for the convergence study (a) coarse and (b) fine. Different meshing for the fluid domain with and without box.

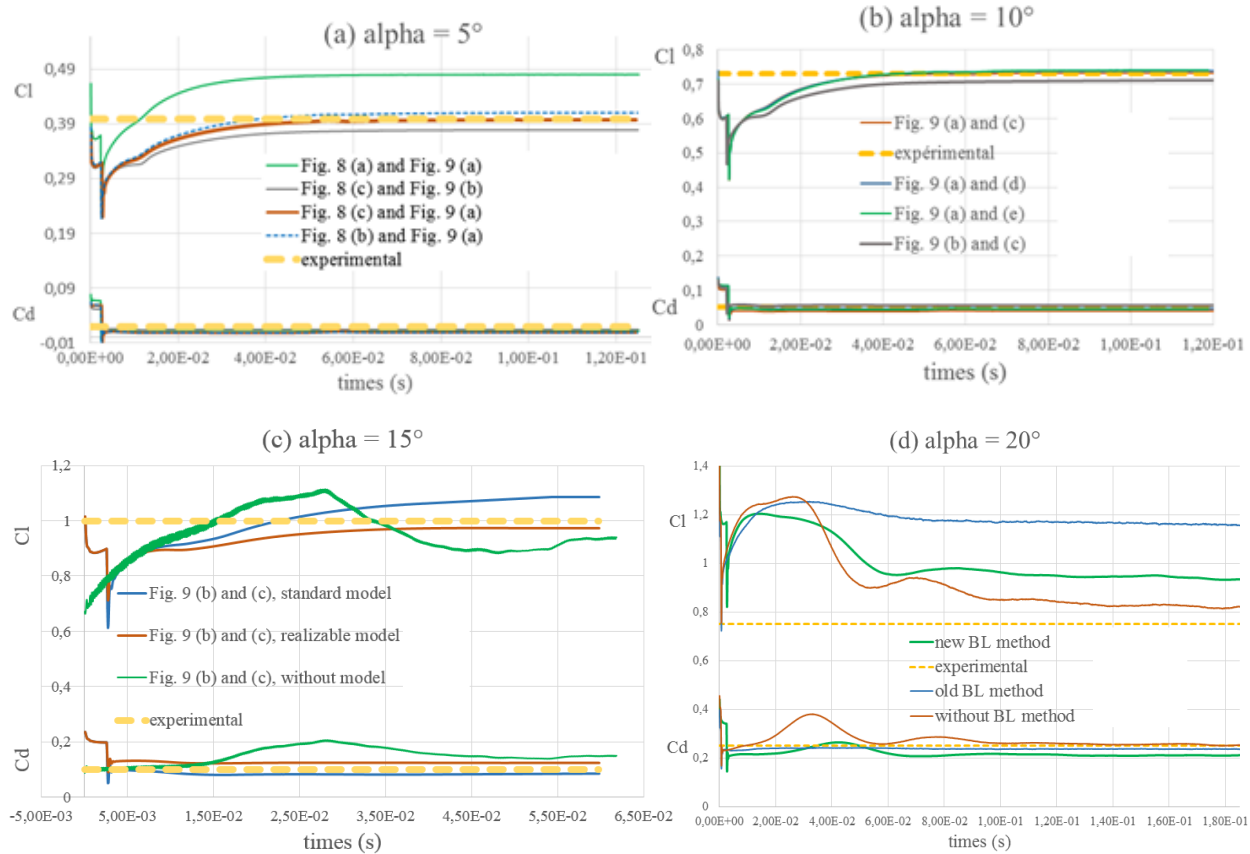
Figure 10 shows the results obtained in 3D to drag and lift at different angle according to different mesh and turbulence model. The higher the angle of attack, the harder it becomes to capture the aerodynamics coefficients.

Figure 10 (a) shows the importance of the size of the domain, in fact the boundary conditions must be away from the obstacle to avoid any artificial constraining of the flow.

Figure 10 (b) shows that when size of the domain and the NACA profile is well discretized (Figure 9 (a)) (cf. paragraph 2.1), the others parameters, such as the presence of a box will allow only to improve results. This conclusion depends on our case study and cannot be generalized. The ICFD solver has a powerful meshing tool which refines the mesh in areas of high gradient. However, this requires very important capacities of memory that may stop the calculation. Moreover, it is not recommended to use important ratio between the refine meshes at the risk of causing errors from the start of calculation.

Figure 10 (c), the presence or absence of a turbulence model has a strong influence on the stability of the calculation. In this case without turbulence model, small vortex are created downstream of the NACA. This is a known effect in the absence of turbulence models. Two turbulence models are compared: the realizable  $k-\varepsilon$  turbulence model which is considered to be an improvement over the standard model [8]. The lift coefficient is better capture with the realizable model, the drag coefficient is better capture with the standard model.

The new method of refinement of the boundary layer allows to choose a specific mesh size and appears to be particularly interesting in more complex cases parachute modeling. The Figure 10 (d) shows the importance of the mesh in the boundary layers. The case study is particularly sensitive to modeling choices in the boundary layer. The optimum parameters with newly developed capacities are used for 2D study.



**Figure 10 – Examples of convergence for the aeronautical coefficients with the ICFD solver: (a) influence of the domain size at  $\alpha=5^\circ$ , (b) influence of meshing near the NACA at  $\alpha=10^\circ$ , (c) influence of the turbulence model at  $\alpha=15^\circ$  and (d) influence of the mesh in the Boundary Layer (BL) at  $\alpha=20^\circ$ .**

From this sensitivity study in 3D, an optimal ICFD model in 2D is set up to compare the aerodynamic coefficients results obtained with the ALE solver and experimental measurements.

### 3 Comparison to experimental

Following the 3D sensitivity studies in ALE and ICFD, the objective of this section is to compare the two solvers in their optimal configuration with experimental results. Due to the symmetry of the problem, the 2D case was chosen for this comparison. For ALE model, a false 2D model was used (a 3D mesh with only 1 element through thickness).

#### 3.1 Velocity shape

On Figure 11, we compare the numerical results obtained with the ALE and ICFD solvers. The results of the 2D models for optimal configurations are presented: the size of the fluid domain and the discretization of NACA are identical.

The ALE model consists of a fluid domain with about 3.4 millions of elements (mesh size around 1mm near NACA profile). For 0.5s physical time (stabilization time), this model takes 24h50 of calculation time in MPP decomposition in 14 procs.

The ICFD model includes 250,000 elements. For 0.1s physical time, this model takes 1h40 of calculation time in MPP decomposition in 14 procs.

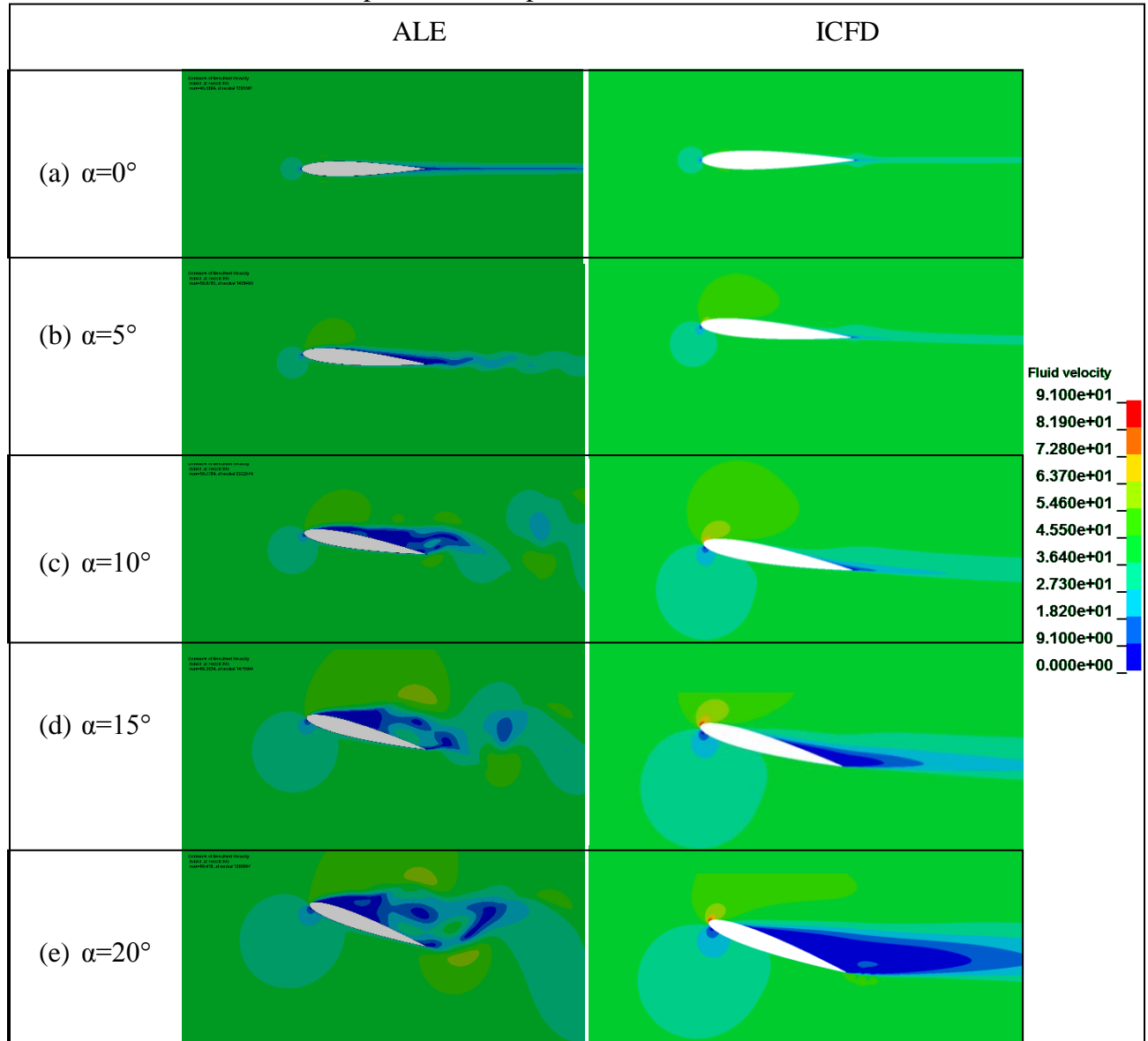


Figure 11 – Velocity field (left) in ALE and (right) in ICFD: (a)  $\alpha=0^\circ$ , (b)  $\alpha=5^\circ$ , (c)  $\alpha=10^\circ$ , (d)  $\alpha=15^\circ$  and (e)  $\alpha=20^\circ$ . Scale: [0; 91] m/s from bleu to red.

The Figure 11 presents a comparison of flow velocity at different the angles of attack of  $0^\circ$ ,  $5^\circ$ ,  $10^\circ$ ,  $15^\circ$  and  $20^\circ$  for the ALE and ICFD solver. The order of magnitude is the same for the two solvers. The main differences correspond to the absence of speed increasing zone at the leading edge of the NACA and the presence of turbillon in the case of the ALE calculations.

In fact in ALE, the difference is visible at the levels of velocity fields in the trail of the wing and in the formation of wing tip vortices. In these areas, disruptions are not extensive in the trail. As the problem is established in perfect fluid and the trailing edge is not imposed as a breakpoint, there are two overlapping flow in the trailing edge: the bypass flow and the circulatory flow.

These different is explained partly by the lack of specific mesh in the high gradient zone (boundary layer in leading edge, the upper area and the trailing edge) for the ALE solver. Plus, there is no concept of distance from the wall but rather a notion of interface through the coupling

method by penalty (no friction, no turbulence model). The latter prevents to calculate the pressure forces properly and to take into account the circulation around the airfoil and in the trailing edge area.

Here, the ALE approach has reached its limits. The solver seems suffer of lacks both on modeling and on the meshing technic to study the flow around an obstacle. The solver does not have either transition model, nor turbulence model and it is not able to reproduce boundary layer phenomena because, on one hand, the dynamic viscosity is not considered and in the other hand, no concept of distance to the wall is set. The meshing technique of submerged boundaries used in the coupling method by penalty is not suitable for this type of problem.

In ICFD, the bypass of the flow is relatively classic: there is this over speed in leading edge region which causes depression and as a result an increase of lift. Following the qualitative analysis, the following paragraph enables a quantitative analysis of the aerodynamic coefficient.

### 3.2 Aerodynamic coefficients

On Figure 12, we compare the experimental results to numerical results obtained with the ALE and ICFD solvers. Two types of experimental results are plot in Figure 8: the ISAE measures and the results from a literature study [9]. In fact in the literature, many authors measure different aerodynamic coefficients for same numbers Reynolds. Figure 12, uncertainty vertical bar summarizes all the experimental values found in the literature [4, 10].

We observe that the ALE solver provides results that are far from tests for lift. It is strongly undervalued. At the numerical level, only the Van Leer method is most suitable to our problem but it requires significant computing power.

The results with the ICFD solver are very promising for the lift and drag coefficient, even if it underestimates the boundary layer separation and it delays the stall. Two turbulence models are compared: the realizable  $k-\epsilon$  turbulence model and the standard model. As in 3D, the lift coefficient is better capture with the realizable model and the drag coefficient is better capture with the standard model.

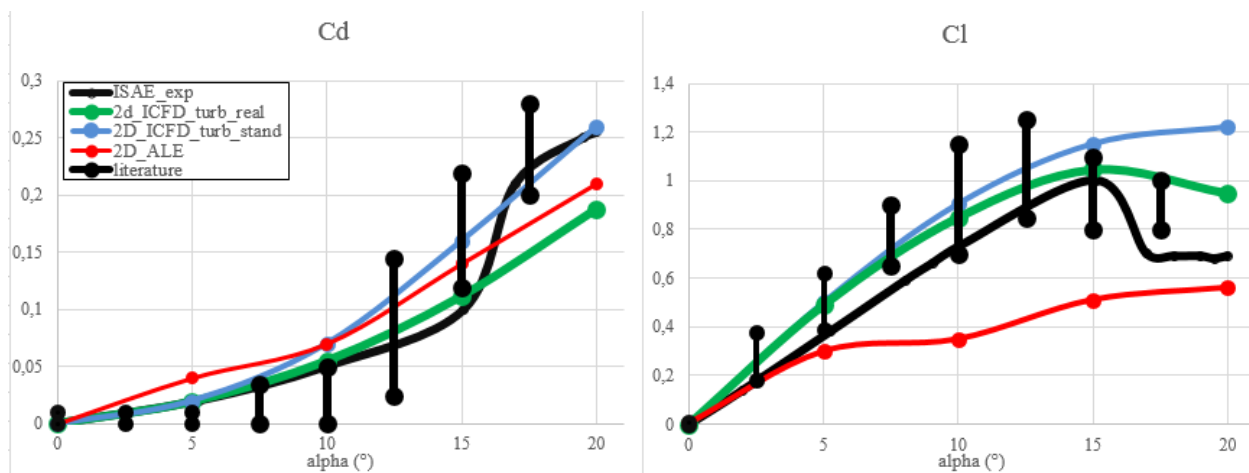


Figure 12 – Comparison of results between experimental, ALE and ICFD solvers on drag-Cd (left), on lift-Cl (right).

Figure 13, for 20° the pressure coefficients  $C_p$ , as  $C_p=2(P-P_{ref})/\rho v^2$ , the two turbulence models are compared. The results for the standard model seem to overestimate the value of the pressure peak on the upper surface. Moreover, the difference between the two models of turbulence occurs at the capture of the stall (lift coefficient in figure 12):

- At 20°, if the standard model detects a recirculation zone at the end of the NACA profile, the localization of it is underestimated. This explains a low decrease in lift curve, but does not correspond to a net stall.
- Conversely, for the realizable model, the recirculation zone is located more upstream, approximately in the first third of the NACA. This explains the inflection of the lift curve: the stall is detected.

This difference is also visible on the curves in Figure 13. On the realizable model, we see that the pressure curve reaches a minimum at a distance of  $X=0.08$  while it is not until  $X=0.17$  to reach the same minimum in the standard model.

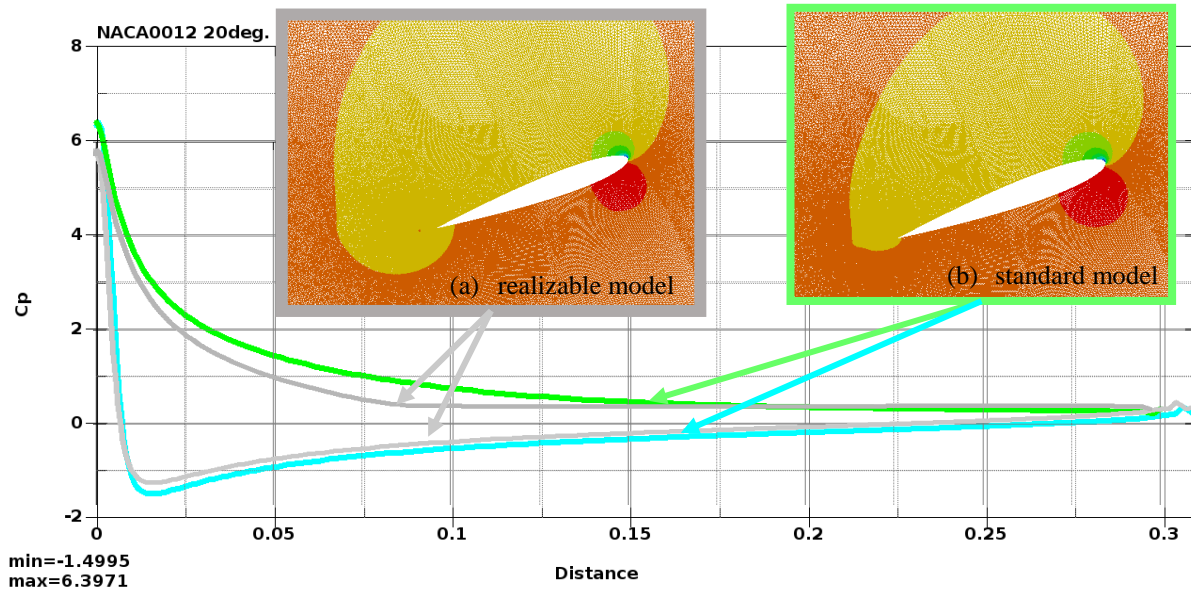


Figure 13 – Comparison of the  $C_p$  for the two turbulence models of the ICFD solver and the level of pressure (a) realizable model and (b) standard model

## Conclusion

The case presented in this paper is representative of the problems addressed by the DGA Aeronautical Systems, the DAEP of ISAE and DynaS+. It has allowed, in a relatively simple case, to compare the performance of ALE and ICFD solver. The results confirmed the optimized capacity of the ICFD solver for this type of FSI study.

Indeed, the aerodynamic behavior study of a wing shown a problem of the type of modelization in ALE. In fact, this solver is designed in a context of problems of fast dynamic modeling of hydrodynamic impact with characteristic times in the range of a millisecond, period for which the viscous phenomena does not have time to be set up. Thus, without taking account of the boundary layer, the viscous coupling and turbulence model, the ALE solver does not correctly capture the aerodynamic coefficients, the level of velocity and pressure.

Compared to the ALE solver, the ICFD solver is presented results in consistent with the experimental measures, while maintaining acceptable computational times. Thus, the ICFD solver is one on which we can rely in the future, notably through the pallet of options of flow models and tools of meshing.

Finally, the next step will be to use this solver ICFD a more representative cases parachutes, especially in the case of flexible structures in order to make full use of the Powerful FSI capabilities of LS-DYNA.

## Acknowledgment

This research was helped by LSTC support and DynaS+ support. We thank N. Acquelet for assistance with the ALE solver and T. Maillot for his work.

## References

- 
- [1] B. Perin, A. Donnard, P. Bordenave, C. Larrieu, C. Simond, "Fluid-Structure Interaction Simulation of Ram Air Parachutes – An Application for a Kite," 23st AIAA Aerodynamic Decelerator Systems Technology Conference and Seminar, Daytona Beach, USA, 2015.
- [2] Coquet Y., Bordenave P., Capmas G., and Espinosa C., "Improvements in Fluid Structure Interaction simulations of parachutes using LS-DYNA," 21st AIAA Aerodynamic Decelerator Systems Technology Conference and Seminar, Dublin, Ireland, 2011.
- [3] Espinosa C., De Lassat de Pressigny Y., Bordenave P., and Henke L., "Fluid-Structure Interaction simulation of parachute dynamic behaviour," 19th AIAA Aerodynamic Decelerator Systems Technology Conference and Seminar, Williamsburg, VA, 2007.
- [4] Gregory N. and C.L. O'Reilly, Low-Speed Aerodynamic Characteristics of NACA 0012 Aerofoil section, including the effect of Upper-Surface roughness Simulating Hoar Frost, R&M No. 3726, London, 1973.
- [5] McCroskey, W. J., "A Critical Assessment of Wind Tunnel Results for the NACA 0012 Airfoil," AGARD CP-429, July 1988
- [6] Codina, R. "Pressure Stability in Fractional Step Finite Element Methods for Incompressible Flows." *Journal of Computational Physics* 170, no. 1 (2001): 112-140.
- [7] Del Pin F., Çaldichoury I., and Paz R. LS-DYNA ICFD Theory Manual. LSTC, 2011.
- [8] Shih T.H, W.W. Liou, A. Shabbir, Z. Yang, and Zhu J. "A New  $k-\epsilon$  Eddy Viscosity Model for High Reynolds Number Turbulent Flows—Model Development and Validation." *Computers Fluids* 24 (1995): 227-238.
- [9] [http://turbmodels.larc.nasa.gov/naca0012\\_val.html](http://turbmodels.larc.nasa.gov/naca0012_val.html)
- [10] Kianoosh Y., Reza Saleh, The effects of trailing edge blowing on aerodynamic characteristics of the Naca 0012 airfoil and optimization of the blowing slot geometry, *Journal Of Theoretical And Applied Mechanics* 52, 1, pp. 165-179, Warsaw 2014